Received: 3 July 2020 | Revised: 18 November 2020 | Accepted: 20 November 2020

DOI: 10.1111/bcpt.13538

ORIGINAL ARTICLE

BCPT Basic & Clinical Pharmacology & Toxicology

Drug-drug interaction of atazanavir on UGT1A1-mediated glucuronidation of molidustat in human

Dorina van der Mey[1] | **Michael Gerisch**[2] | **Natalia A. Jungmann**[2] | **Andreas Kaiser**[3] | **Kenichi Yoshikawa**[4] | **Simone Schulz**[2] | **Martin Radtke**[2] | **Silvia Lentini**[1]

[1]Clinical Pharmacology Cardiovascular/Haematology, Translational Sciences, Research & Development, Bayer AG, Wuppertal, Germany

[2]Drug Metabolism and Pharmacokinetics, Translational Sciences, Research & Development, Bayer AG, Wuppertal, Germany

[3]Statistics and Data Insights, Data Sciences & Analytics, Research & Development, Bayer AG, Berlin, Germany

[4]Clinical Pharmacology, Clinical Sciences, Research & Development, Bayer Yakuhin Ltd, Osaka, Japan

Correspondence
Dorina van der Mey, Clinical Pharmacology Cardiovascular/Haematology, Translational Sciences, Research & Development, Aprather Weg 18a, 42113 Wuppertal, Germany.
Email: dorina.vandermey@bayer.com

Funding information
Bayer AG

Abstract

Molidustat is an oral inhibitor of hypoxia-inducible factor (HIF) prolyl-hydroxylase enhancing the erythropoietin (EPO) response to HIF; it is in clinical development for the treatment of anaemia related to chronic kidney disease. The predominant role of glucuronidation for molidustat clearance (formation of N-glucuronide metabolite M1) and subsequent renal excretion was confirmed in a human mass balance study, with about 85% of the drug being excreted as M1 in urine. The inhibitory effects of 176 drugs and xenobiotics from various compound classes on the UGT-mediated glucuronidation of molidustat in human liver microsomes (HLMs) were investigated. Based on preclinical findings, glucuronidation of molidustat was predominantly mediated by the 5'-diphospho-glucuronosyltransferase (UGT) isoform UGT1A1. Therefore, atazanavir, which is a potent inhibitor of UGT1A1, was chosen for the evaluation of pharmacokinetics and EPO release following a single oral dose of 25 mg molidustat. Molidustat exposure increased about twofold upon coadministration with atazanavir when considering area under plasma concentration-time curve from zero to infinity (AUC) and maximum plasma concentration (C_{max}). Baseline-corrected increase of EPO was 14% and 34% for C_{max} and AUC (calculated over 24 hours), respectively. Coadministration of molidustat and atazanavir was well tolerated.

KEYWORDS

atazanavir, drug-drug interaction, HIF-PH inhibitor, molidustat, UGT

1 | INTRODUCTION

Anaemia is a common complication of chronic kidney disease (CKD). This is partly caused by impairment of physiological hypoxia detection at the renal level and the corresponding release of hypoxia-induced factors (HIFs).[1,2] In the presence of oxygen, HIF-α subunits are tagged by proline hydroxylation for deactivation by HIF proline hydroxylase,[3,4] which reduces erythropoietin (EPO) expression. Molidustat has been shown to inhibit HIF-PH (EC 1.14.11.29) in the nanomolar concentration range,[5] resulting in sustained physiological transcription of the *EPO* gene. This, in turn, leads to increased EPO release and increased haemoglobin concentrations in patients with CKD, as established in the phase 2 DIALOGUE trials.[1]

Clinical intervention in renal anaemia via erythropoiesis-stimulating agents (ESAs), the standard treatment in CKD-related anaemia since 1989, has well-known disadvantages. These include the parenteral administration of

the protein drugs, primary/secondary resistance (in ~10%-20% of patients) and potential cardiovascular side effects (eg increased risk of cardiovascular disease and death).[1,6-8] Therefore, the stabilization of HIFs, which are the primary physiological signal for hypoxia-induced increase in erythropoiesis, is a new and promising clinical pathway for the management of CKD-induced anaemia.[4,5,9-11]

The molidustat pharmacokinetic (PK) profile, including the metabolic fate and routes of excretion, has been studied in humans following oral administration. Molidustat was almost completely absorbed from the gastrointestinal tract and had an absolute oral bioavailability of about 60%. Molidustat is subsequently cleared extensively via conjugation, resulting in the N-glucuronide metabolite M1; this metabolite undergoes renal elimination, with about 85% of the administered dose being recovered as M1 in urine. Only a minor fraction of the dose is excreted as molidustat via urine (~4%) or faeces (~6%).[2,12] Based on the high relevance of glucuronidation for the molidustat PK profile, the uridine 5'-diphospho-glucuronosyltransferase (UGT) isoforms involved had to be identified and subsequently screened for potential drug-drug interactions (DDIs) with co-medications or food. Based on these findings, atazanavir was chosen as a model compound to be tested in a clinical DDI study evaluating the influence of a strong UGT1A1 inhibitor on the PK and pharmacodynamic (PD) profiles of molidustat. In the following paper, the results from the DDI study for molidustat with repeated doses of atazanavir are reported. The data from UGT isoform identification and in vitro screening for potential interaction partners, which guided the selection of atazanavir as co-medication for the clinical study, are also presented.

2 | METHODS

The study was conducted in accordance with the Basic & Clinical Pharmacology & Toxicology policy for experimental and clinical studies.[13]

2.1 | Identification of relevant UGT isoforms

2.1.1 | Isoform-expressing microsomes

In a first step, 12 human UGTs expressed in insect cells (ie UGT1A1, 1A3, 1A4, 1A6, 1A7, 1A8, 1A9, 1A10, 2B4, 2B7, 2B15, 2B17; Supersomes, BD Gentest, Woburn, MA, USA), as well as microsomes from non-transfected control insect cells, were screened for the catalytic activity for the formation of the N-glucuronide of molidustat (M1), the major human metabolite. For this, [^{14}C]molidustat was incubated at final concentrations of 1.0 µmol L^{-1} and 10 µmol L^{-1}, with 0.5 mg mL^{-1} microsomal protein in the presence of alamethicin (50 µg mg^{-1} protein), after 15 minutes of preincubation on ice. Incubations (N = 1) were performed in 100 mmol L^{-1} potassium phosphate buffer (pH 7.4), containing 5 mmol L^{-1} magnesium chloride. After addition of molidustat and saccharolactone (5 mmol L^{-1}), the solution was pre-warmed to 37°C for 5 minutes, and the reaction was started subsequently by adding uridine 5'-diphosphoglucuronic acid (UDPGA) at a final concentration of 5 mmol L^{-1}. After 30 minutes or 60 minutes at 37°C, the reaction was terminated by addition of 5% phosphoric acid/acetonitrile (1:10) and cooled on ice. After centrifugation, supernatants were injected onto a high-performance liquid chromatographic (HPLC) system (HP1100, Agilent) with off-line radioactivity detection (Wallac 1450 MicroBeta, PerkinElmer/Wallac) using Ultima Flo AP scintillation fluid (PerkinElmer/Canberra Packard). For incubations with low molidustat concentration (1.0 µmol L^{-1}), samples were concentrated under reduced pressure prior to HPLC analysis. Chemicals were purchased from Fluka or Sigma, or Merck, if not mentioned otherwise.

2.1.2 | Isoform-specific inhibitor experiments

In a second step, microsomes from the human liver (Cytonet), intestine or kidney (XenoTech) were incubated (N = 2, arithmetic means presented) with molidustat (4.9 µmol L^{-1}) under essentially the same conditions as described above at a final protein concentration of 0.5 mg mL^{-1}. Isoform-specific inhibitors of UGTs were added before initiating the reaction with UDPGA; these inhibitors were 5 µmol L^{-1} atazanavir (inhibitor of UGT1A1),[14] 10 µmol L^{-1} hecogenin (inhibitor of UGT1A4,),[15] 5 µmol L^{-1} niflumic acid (inhibitor of UGT1A9) [16,17] or 10 µmol L^{-1} mefenamic acid (inhibitor of UGT2B7, at higher concentrations also UGT1A9).[18]

2.1.3 | Kinetic parameters

In order to determine enzyme kinetic parameters of the glucuronidation reaction in human liver microsomes, [^{14}C] molidustat was incubated at concentrations of 2.4, 4.9, 9.9, 24.9, and 49.1 µmol L^{-1} (N = 2, Table S1). The experimental conditions were identical as described for isoform-specific inhibitor experiments. For the determination enzyme kinetic parameters of the glucuronidation reaction in recombinant UGT1A1 and UGT1A9, [^{14}C]BAY 85-3934 was incubated at a concentration of 2.4, 4.9, 9.9, 24.9, 49.1 and 96.6 µmol L^{-1} (N = 2, Tables S2 and S3). The experimental conditions were identical as described for isoform-expressing microsomes. Enzyme kinetic fits were performed by non-linear regression analysis using SigmaPlot software (version 11). For human liver microsomes and UGT1A1, the data were fit

to the Hill equation, and for UGT1A9, the data were fit to the conventional Michaelis-Menten equation.

2.1.4 | Correlation analysis

To further elaborate the contribution of UGT1A1 and UGT1A9 to the glucuronidation of molidustat, molidustat was incubated with 23 individual human liver microsomal preparations and one sample of pooled human liver microsomes (HLMs), which had been characterized in parallel for their enzymatic activity for two UGT isoform-specific substrates (ie 17β-estradiol to 17β-estradiol 3-glucuronide [UGT1A1] and propofol to β-D-glucuronide [UGT1A9]). Incubations (N = 2, arithmetic means presented) were performed as described above for microsomal experiments with UGT isoform-specific inhibitors, using molidustat (5 µmol L^{-1}), 17β-estradiol (20 µmol L^{-1}) [19] or propofol (100 µmol L^{-1}),[20,21] 0.3 mg mL^{-1} protein and 15-30-minute incubation times. Samples were analysed for M1, 17β-estradiol 3-glucuronide or propofol glucuronide via HPLC mass spectrometry (HP1100 or HP1290, Agilent, and AB SCIEX API3200 or API 4000, AB Sciex Pte. Ltd.). M1-d8 (in-house synthesis) or naphthol glucuronide (Sigma-Aldrich) served as the internal standards. Velocity of molidustat glucuronidation was correlated to respective isoform-specific activity for UGT1A1 (17β-estradiol 3-glucuronidation) and UGT1A9 (propofol glucuronidation) using linear regression analysis.

2.2 | Screening for potential DDI interactions

Incubations (N = 1; 30 minutes) with pooled HLMs (0.3 mg mL^{-1}) were performed as described above, with molidustat (5 µmol L^{-1}) (total volume: 200 µL) in the presence of six different concentrations for 176 xenobiotics (obtained from commercial suppliers; see Table 1 and Table S4) to determine the inhibitory potency and, if applicable, half maximal inhibitory concentration (IC_{50}) values for inhibition of M1 formation from molidustat. Incubations without inhibitor served as controls and in each run of 14 putative inhibitors atazanavir served as positive control. Experiments were performed on a Genesis Workstation (Tecan) or a Microlab STARlet (Hamilton Robotics). Reactions were terminated by addition of acetonitrile/formic acid (10:1) containing internal standard M1-d8. After centrifugation, supernatants were analysed by liquid chromatography-tandem mass spectrometry (LC-MS/MS) for quantification of M1 as described above. Linear interpolation was used to determine IC_{50} values. If less than 50% inhibition was observed, data were not extrapolated. To identify potentially relevant interaction partners for

TABLE 1 Inhibitory potential (IC_{50}) of various compounds on molidustat glucuronidation in pooled human liver microsomes and estimated increase in molidustat AUC

Inhibitor	IC_{50}, µmol L^{-1}	$AUCR_{inlet}$, k_a 0.1 min^{-1}	$AUCR_{inlet}$, k_a 0.01 min^{-1}
Erlotinib	0.13	7.26	4.54
Nilotinib	0.17	5.10	2.03
Sorafenib	0.32	3.01	1.74
Atazanavir	0.42	6.29	3.44
	0.42	2.91[a]	2.44[b]
Saquinavir	0.47	3.18	1.32
Montelukast	0.49	1.04	1.02
Ritonavir	0.60	1.83	1.38
Tacrolimus	0.70	1.01	1.01
Itraconazole	1.2	1.03	1.00
Lopinavir	1.3	1.52	1.19
Dasatinib	1.4	1.13	1.02
Mifepristone	1.4	2.06	1.16
Axitinib	1.5	1.01	1.00
Nelfinavir	1.5	1.72	1.12
Bilirubin	1.5	n.c.	n.c.
Tranilast	1.7	4.37	3.65
Nifedipine	1.7	1.04	1.01
Gefitinib	1.8	2.61	1.22
Curcumin	2.2	n.c.	n.c.
Genistein	2.3	n.c.	n.c.
Raloxifene	2.3	1.18	1.02
Lapatinib	2.5	1.58	1.07
Atorvastatin	2.6	1.06	1.01
Telmisartan	2.8	1.02	1.00
Carvedilol	2.9	1.03	1.01
Indinavir	3.0	5.59	2.61
Cisapride	4.1	1.01	1.00
Domperidone	4.3	1.15	1.02
Rifampicin	4.3	4.15	2.26
Everolimus	4.5	1.20	1.02
Cyclosporin	4.9	1.24	1.04
(-)-Epigallocatechin	5.1	n.c.	n.c.
Quercetin	5.5	n.c.	n.c.
Ketoconazole	6.1	1.04	1.01
Glibenclamide	6.3	1.00	1.00
Daidzein	6.8	n.c.	n.c.
Febuxostat	7.2	1.03	1.02
Efavirenz	8.0	1.05	1.01
Imatinib	9.4	1.25	1.05

(Continues)

TABLE 1 (Continued)

Inhibitor	IC_{50}, µmol L^{-1}	$AUCR_{inlet}$, k_a 0.1 min^{-1}	$AUCR_{inlet}$, k_a 0.01 min^{-1}
Clotrimazole	10.2	2.90	1.26
Docetaxel	10.5	1.08	1.02
Lovastatin	10.5	1.05	1.01
Celecoxib	10.6	1.09	1.01
Rosiglitazone	10.7	1.00	1.00
17a-Ethynylestradiol	10.8	1.00	1.00
Paclitaxel	10.8	1.21	1.03
Midazolam	11.1	1.01	1.00
Nefazodone	11.4	1.02	1.01
Naringenin	11.6	n.c.	n.c.
Mevastatin	13.2	n.c.	n.c.
Fluvastatin	13.4	1.00	1.00
Verapamil	14.1	1.23	1.03
Niflumic acid	14.6	1.77	1.22
Bergamottin	14.8	n.c.	n.c.
Pitavastatin	14.8	1.00	1.00
Simvastatin	15.1	1.02	1.00
Mefenamic acid	16.0	2.57	1.57
Omeprazole	17.1	1.02	1.00
Droperidol	17.3	n.c.	n.c.
Loperamide	17.9	1.00	1.00
Sunitinib	18.7	1.02	1.00
Miconazole	19.3	n.c.	n.c.
Pantoprazole	19.7	1.01	1.01
Mibefradil	20.2	1.00	1.00
Astemizole	23.5	1.00	1.00
Sulfinpyrazone	31.4	1.04	1.03
Diazepam	34.8	1.00	1.00
Lansoprazole	36.8	1.00	1.00
Sulindac	37.5	1.55	1.09
Diclofenac	38.2	1.00	1.00
Doxorubicin	40.4	1.01	1.01
Androsterone	44.0	n.c.	n.c.
Sildenafil	46.2	1.00	1.00
Amiodarone	49.7	1.00	1.00
Diflunisal	75.6	1.10	1.09
Gemfibrozil glucuronide	96.1	n.c.	n.c.

Note: $AUCR_{inlet}$ (k_a 0.1 min^{-1}) is the increase based on hepatic inlet concentration, assuming a default k_a of 0.1 min^{-1}, and is calculated as $[I]_{inlet,unbound} = f_{u,p} \times \left([I]_{max} + \frac{dose \times F_a \times k_a}{Q_h \times R_B}\right)$, in which $f_{u,p}$ is the unbound fraction in plasma; $[I]_{max}$ is the maximal total (free and bound) inhibitor concentration in plasma at steady state; F_a is the fraction absorbed after oral administration (as worst-case scenario set to 1 if no data available); k_a is the first-order absorption rate constant in vivo, assuming a default value of 0.1 min^{-1} as suggested by guidelines [22] and a less conservative value of 0.01 min^{-1}; Q_h is the hepatic blood flow (ie 97 L/h per 70 kg body weight) [26,27]; and R_B is the blood-to-plasma concentration ratio (set to 1 if no data available).

AUC, area under plasma concentration-time curve from zero to infinity; AUCR, area under plasma concentration-time curve from zero to infinity in the presence of the respective co-medication; IC_{50}, half maximal inhibitory concentration; n.c., not calculated. *Ki* = IC50, since the concentration of molidustat (5 µmol L^{-1}) investigated was far less than the estimated K_m (90 µmol L^{-1}) in human liver microsomes.

[a]Based on $f_m = 0.7$, considering clearance via UGT1A1 only and k_a value of 0.108 min^{-1}.[29]

[b]Based on $f_m = 0.7$, considering clearance via UGT1A1 only and k_a value of 0.024 min^{-1}.[29]

molidustat glucuronidation (clearance), the predicted increase in molidustat area under plasma concentration-time curve from zero to infinity (AUC) in the presence of the respective co-medication (AUCR) was calculated according to scientific[22,23] and regulatory proposals[24,25] using the following formula.

Fraction metabolized via total glucuronidation (f_m) was ~0.9, based on results from the mass balance study (upper limit of sum of N-glucuronide in urine [85%] and molidustat in faeces [~6%], possibly resulting from hydrolysis in gastrointestinal tract from biliary-excreted M1) without differentiating between UGT1A1 and UGT1A9 in M1 formation. [*I*] represents the in vivo concentration of the inhibitor available to inhibit glucuronidation of molidustat. The value for [*I*] should ideally represent the concentration of inhibitor at the site of the UGT isoform in the liver cells because, based on the absolute bioavailability study, the liver is by far the predominant site of molidustat glucuronidation.[12] According to guidelines from the European Medicines Agency and the US Food and Drug Administration,[24,25] the maximum unbound concentration at the inlet to the liver ($[I]_{inlet,u}$) was used[22] (for calculation see Table S5).

$$[I]_{inlet,u} = f_{u,p} \times \left([I]_{max} + \frac{dose \times F_a \times k_a}{Q_h \cdot R_B}\right).$$

$$AUCR = \frac{1}{\frac{f_m}{1+\frac{[I]}{k_i}} + (1 - f_m)}$$

$f_{u,p}$ is the unbound fraction in plasma; $[I]_{max}$ is the maximal total (free and bound) inhibitor concentration in plasma at steady state; F_a is the fraction absorbed after oral administration (as worst-case scenario set to 1 if no data available); k_a is the first-order absorption rate constant in vivo, assuming a default value of 0.1 min^{-1}, as suggested by guidelines,[22] and a less conservative value of 0.01 min^{-1}; Q_h is the hepatic blood flow (ie 97 L h^{-1} per 70 kg body weight)[26,27]; and R_B is the blood-to-plasma concentration

ratio (set to 1 if no data available). Based on $K_i = IC_{50}/(1 + [I]/K_m)$, $K_i \sim IC_{50}$ since the glucuronidation of molidustat was performed at a substrate concentration of 5 µmol L^{-1}, which is far less than the estimated K_m value of the glucuronidation of molidustat in human liver microsomes (K_m = 90 µmol L^{-1}). Therefore, the obtained IC_{50} values were used for the calculations.

2.3 | Clinical DDI study design

2.3.1 | Study conduct

Ethics

All participants provided written informed consent prior to entry to the study, which was conducted in accordance with the latest revised version of the Declaration of Helsinki and the International Council for Harmonisation of Technical Requirements for Pharmaceuticals for Human Use guidelines for Good Clinical Practice. The protocol was reviewed and approved by the Ethics of the North-Rhine Medical Council (Düsseldorf, Germany) and by the Federal Institute for Drugs and Medical Devices (BfArM) before study initiation (EudraCT number: 2015-000109-37).

Study design

This was a single-centre, open-label, fixed-sequence, non-placebo-controlled study in healthy, male participants. In the first period, a single immediate-release (IR) tablet of 25 mg molidustat was given with 240 mL of water 2 hours after a standardized, light breakfast consisting of a bread roll, 20 g butter, 25 g jam and 250 mL coffee substitute or fruit tea. Following a washout of at least 72 hours, in the second period, the participants received 400 mg atazanavir (2 × 200 mg Reyataz, Bristol-Myers Squibb) about 30 minutes after a light breakfast for 5 days, and, on the last day, a single IR tablet of 25 mg molidustat was given 1.5 hours after intake of atazanavir.

Study participants

The participants had to be healthy, male individuals who were 18-45 years of age, with a body mass index of at least 18 kg m^{-2} and no higher than 29.9 kg m^{-2}. They could not have any known acute or chronic diseases (especially cardiovascular, renal or hepatic), hypersensitivity to study drugs or excipients, or other severe allergies, and they must not have received acute or chronic medications (including St. John's Wort or grapefruit) in the past 7 days before study medication (especially medications that are contraindicated with atazanavir or drugs that increase gastric pH) or have participated in other clinical studies in the past 3 months or during the current study. Participants who regularly smoked more than 25 cigarettes or consumed more than 20 g of alcohol a day were also excluded.

Safety evaluations

The safety and tolerability parameters included body temperature, blood pressure, heart rate, 12-lead electrocardiogram (ECG), standard laboratory evaluation of blood and urine parameters, as well as reporting of adverse events (AEs).

PK sampling for molidustat (both treatments)

Blood sampling was performed at 0, 0.25, 0.5, 0.75, 1, 1.5, 2, 3, 4, 6, 8, 10, 12, 24, 28, 32, 36 and 48 hours after the dose for characterization of molidustat PK.

PK sampling for atazanavir (second treatment only)

For characterization of atazanavir PK, blood samples were obtained on all 5 study days of the second period prior to administration of atazanavir, as well as on the day of molidustat coadministration 0.5, 1, 1.5, 2, 2.5, 3, 4.5, 5.5, 7.5, 9.5, 13.5, 24, 29.5, 37.5 and 49.5 hours after administration of atazanavir. All samples were stored below −18°C (molidustat) or −80°C (atazanavir) and analysed within 120 days or 39 days after sampling, respectively.

PD sampling

Blood samples for determination of EPO concentrations were collected prior to molidustat administration and 4, 6, 8, 10, 12 and 24 hours after molidustat dosing.

2.3.2 | Analytical methods

Molidustat and metabolite M1

Plasma concentrations were measured after protein precipitation with acetonitrile/water/trifluoroacetic acid using a validated LC-MS/MS method for the concentration range of 0.2-200 µg mL^{-1}, as described before.[2] For molidustat, quality control (QC) samples in the concentration range of 0.500-160 µg L^{-1} and dilution QC samples of 4000 µg L^{-1} (not required in all batches) were determined with an accuracy of 102%-108% and a precision of 3.11%-4.29%. For M1, QC samples in the concentration range of 0.500-160 µg L^{-1} and dilution QC samples of 4000 µg L^{-1} (not required in all batches) were determined with an accuracy of 96.1%-101% and a precision of 2.56%-6.82%.

Atazanavir

Quantitative analysis of atazanavir in plasma was performed using a fully validated, triple quadrupole LC-MS/MS assay ranging from 10 µg mL^{-1} to 10 000 µg mL^{-1}. Following automated protein precipitation and addition of the internal standard (atazanavir-d_5), an aliquot of 50 µL was injected into the liquid chromatographic system with detection in positive TurboIonSpray mode. QC samples in the concentration range of 30-7500 µg L^{-1} were determined with an accuracy of 98.0%-103% and a precision of 1.43%-2.88%.

EPO

The serum concentrations of EPO were measured by a solid-phase, two-site, one-cycle chemiluminescent enzyme immunometric assay (IMMULITE, Siemens Healthcare Diagnostics), as outlined previously.[2]

2.3.3 | Pharmacokinetic evaluation

Non-compartmental analysis of plasma concentration-time data was performed using WinNonlin (Version 6.2.1, Certara) and SAS version 9.3 (SAS Institute). Primary PK parameters were maximum plasma concentration (C_{max}) and AUC of molidustat; additionally, clearance (molidustat only), terminal half-life, time to C_{max} (t_{max}) and area under plasma concentration-time curve from zero to the time of the last quantifiable concentration (AUC[0-t_{last}]) were determined for both molidustat and M1.

2.3.4 | Pharmacodynamic evaluation

The concentration of EPO over time was measured. C_{max}, t_{max} and AUC(0-24) of EPO were calculated to describe the PD effect of molidustat. Moreover, C_{max} of EPO was also calculated based on the ratio and the difference to baseline, and AUC(0-24) based on the difference to baseline.

2.3.5 | Sample size—statistical analysis

For determination of sample size, a priori knowledge on relevant variability of target parameters for molidustat was obtained from previous clinical studies. Assuming a coefficient of variation (CV) for intraindividual variability of less than 20% for AUC and less than 52% for C_{max}, a data set of at least 10 participants available for evaluation would result in a point estimate that deviates from the true ratio 1.16-fold or less (upper bound of 90% range for expected DDI ratio estimate) for AUC and 1.42-fold for C_{max}. To account for potential drop-outs, it was planned to randomize approximately 15 participants.

The safety population included all participants receiving at least one dose; the populations for PK and PD analyses included all participants completing both treatments with valid data sets for PK and PD samples, respectively. PK and PD data were summarized by descriptive statistics.

Moreover, PK parameters (AUC, AUC(0-t_{last}) and C_{max} of molidustat and M1, as well as AUC(0-24) and C_{max} of EPO data (absolute concentrations and ratio to baseline for C_{max} and difference to baseline for AUC), were analysed using analysis of variance (ANOVA). Assuming log normally distributed data, the ANOVAs were performed on log-transformed data. Point estimates for the DDI ratios (molidustat + atazanavir)/molidustat, derived from differences of least-squares means, as well as exploratory 90% confidence intervals, were calculated. No confirmatory statistical analysis was intended.

3 | RESULTS

3.1 | In vitro studies

3.1.1 | Identification of relevant UGT isoform(s)

Of the human UGT isoforms tested, only UGT1A1 and UGT1A9 had considerable catalytic activity for the formation of M1; molidustat velocities for M1 formation were 13.0 and 5.99 pmol/(mg recombinant microsomal protein × min) at a concentration of 1 µmol L^{-1}, and 115 and 39.1 pmol/(mg recombinant microsomal protein × min) at a concentration of 10 µmol L^{-1}, respectively. Isoforms UGT1A3, 1A7 and 1A8 revealed low activities of 0.79, 1.22 and 0.82 pmol/(mg recombinant microsomal protein × min) at a concentration of 1 µmol L^{-1} and of 5.9, 5.8 and 6.8 pmol/(mg recombinant microsomal protein × min) at a concentration of 10 µmol L^{-1}, respectively, while the remaining isoforms (ie UGT1A4, 1A6, 1A10, 2B4, 2B7, 2B15, 2B17) lacked measurable activity for glucuronidation of molidustat. To assess the relative contribution of UGT isoforms to metabolic activity in microsomal preparations, the inhibitory effects of the isoform-specific inhibitors atazanavir (UGT1A1) and niflumic acid (UGT1A9) were studied in human microsomes prepared from the liver, intestine and kidney. Without an inhibitor, the catalytic activity for glucuronidation was highest in liver microsomes (~55 pmol M1/[mg liver microsomal protein × min]) compared with intestinal microsomes (~23 pmol M1/[mg intestinal microsomal protein × min]) or kidney microsomes (~12 pmol M1/[mg kidney microsomal protein × min]; data not shown). The effect of both inhibitors was most pronounced in liver microsomes and was considerably higher for 5 µmol L^{-1} atazanavir (~70% reduction in formation of M1) than for 5 µmol L^{-1} niflumic acid (~25% reduction), as shown in Table 2. In addition, 10 µmol L^{-1} hecogenin and 10 µmol L^{-1} mefenamic acid displayed none or very little activity in liver, intestine and kidney microsomes (Table 2).

The concentration dependence of M-1 formation was investigated with human liver microsomes (Table S1) and with UGT1A1 (Table S2) as well as with UGT1A9 (Table S3). Determination of apparent K_m or S_{50} and V_{max} values was not possible as the affinity of molidustat seems to be low towards enzyme preparations tested, and V_{max} values could not be reached up to a substrate concentration of 96 µmol L^{-1}. The estimated S_{50} values for human liver microsomes and UGT1A1 are 90 µmol L^{-1} and about 200 µmol L^{-1},

respectively. The estimated K_m value for UGT1A9 is about 200 μmol L^{-1}. To further clarify the relative contribution of UGT1A1 and UGT1A9 to molidustat (5 μmol L^{-1}) glucuronidation activity, single-donor HLMs (N = 23) and one batch of pooled HLMs were characterized for isotype-specific glucuronidation capacity, using 20 μmol L^{-1} 17β-estradiol (17β-estradiol 3-glucuronidation, UGT1A1) and 100 μmol L^{-1} propofol (propofol glucuronidation, UGT1A9) as model substrates (Table S4). Subsequently, enzymatic activities for the two isoforms were correlated by linear regression analysis to the enzymatic activity for formation of M1, as depicted in Figure 1. A strong correlation was observed for M1 formation and UGT1A1 activity (17β-estradiol 3-glucuronidation), with an r^2 of 0.902; for propofol glucuronidation reflecting UGT1A9 activity, the correlation was much less pronounced (r^2: 0.511). Based on these results, it was concluded that hepatic UGT1A1 was the predominant enzyme responsible for M1 formation in humans, with minor involvement of UGT1A9.

3.1.2 | Screening for potential DDIs

The inhibitory effects of 176 drugs and xenobiotics from various compound classes (eg anticancer drugs, analgesics, antivirals, antibiotics, antifungals) on the UGT-mediated glucuronidation of molidustat in HLMs were investigated and assessed based on IC_{50} values. Results obtained are presented in Table 1 and Table S6, including the respective IC_{50} values and calculated impact on change in AUC of molidustat (AUCR) using different approximations (if applicable). The most efficient inhibitors, with IC_{50} values in the nanomolar concentration range, were the kinase inhibitors erlotinib (0.13 μmol L^{-1}), nilotinib (0.17 μmol L^{-1}) and sorafenib (0.32 μmol L^{-1}), but the well-known UGT1A1 inhibitor atazanavir also exhibited high potency (0.42 μmol L^{-1}), followed by saquinavir (0.47 μmol L^{-1}), montelukast (0.49 μmol L^{-1}), ritonavir (0.60 μmol L^{-1}) and tacrolimus (0.70 μmol L^{-1}). A number of compounds exhibited half-maximum inhibitory activity in the range of 1-10 μmol L^{-1}, such as itraconazole (IC_{50}: 1.2 μmol L^{-1}), bilirubin (1.5 μmol L^{-1}), additional tyrosine kinase inhibitors (axitinib, dasatinib, gefitinib, imatinib, lapatinib), human immunodeficiency virus (HIV) protease inhibitors (indinavir, lopinavir, nelfinavir), and atorvastatin, carvedilol, cisapride, curcumin, cyclosporin, daidzein, domperidone, epigallocatechin, everolimus, febuxostat, genistein, glyburide (glibenclamide), ketoconazole, mifepristone, nifedipine, quercetin, raloxifene, rifampicin, telmisartan efavirenz and tranilast.

An in vitro-in vivo scaling approach was used to estimate the AUCR for molidustat based on a conservative f_m of 0.9 (glucuronidation of molidustat without differentiation via specific UGTs), using for the perpetrator drugs unbound inlet concentration with default k_a values of 0.1 min^{-1} and 0.01 min^{-1} (Table 1). Since the glucuronidation of molidustat was performed at a substrate concentration of 5 μmol L^{-1}, which is far less than the estimated K_m value of the glucuronidation of molidustat in human liver microsomes (90 μmol L^{-1}) K_i equals to IC_{50} ($K_i = IC_{50}/(1+[I]/K_m)$). Therefore, the IC_{50} values obtained were used for the calculations.

Using this approach, an increase in AUC of more than fivefold was predicted for the kinase inhibitors erlotinib and nilotinib, and the antiretrovirals atazanavir and indinavir. It is worth noting that none of the substances tested were predicted to be strong inhibitors of molidustat glucuronidation when using a lower k_a value of 0.01 min^{-1} corresponding to a slower absorption rate.

For most of the compounds tested (about 130), no risk of potential DDI in vivo was assumed, based on an increase in molidustat AUC of less than 25% (AUCR < 1.25) and/or a lack of relevant inhibitory activity detected (Table 1 and Table S6). This group of test compounds included widely used drugs such as analgesics (acetaminophen, diclofenac, ibuprofen), cardiovascular drugs (eg atorvastatin, simvastatin, fluvastatin, lovastatin, rosuvastatin, candesartan, metoprolol, carvedilol, verapamil, nifedipine, clopidogrel, ticlopidine, warfarin), proton pump inhibitors (omeprazole, lansoprazole), oral antidiabetics (rosiglitazone, glyburide, tolbutamide) or potential concomitant immunosuppressant medications (eg cyclosporine, tacrolimus, everolimus, dexamethasone).

For atazanavir, the effect on molidustat AUC was calculated for glucuronidation via UGT1A1 only, given that the inhibitory potency on UGT1A9 was much less pronounced.[28] The f_m value of approximately 0.7 via UGT1A1 was estimated based on the total fraction excreted via glucuronidation (f_m: 0.9), and the remaining activity in the HLMs incubated

TABLE 2 Influence of different standard UGT inhibitors on formation of molidustat glucuronide M1 in pooled human microsomes prepared from different tissues (n = 2 each)

	M1 formation in % of control in microsomal tissue		
Inhibitor/UGT isoform	**Intestine**	**Liver**	**Kidney**
Control	100	100	100
5 μmol L^{-1} atazanavir/ UGT1A1	24.8	31.7	98.8
10 μmol L^{-1} hecogenin/ UGT1A4	106.0	104.7	102.4
5 μmol L^{-1} niflumic acid/ UGT1A9	91.0	76.3	19.5
10 μmol L^{-1} mefenamic acid/ UGT2B7(+UGT1A9)	87.0	91.5	70.6

Note.: -, not applicable; UGT, uridine 5'-diphospho-glucuronosyltransferase.

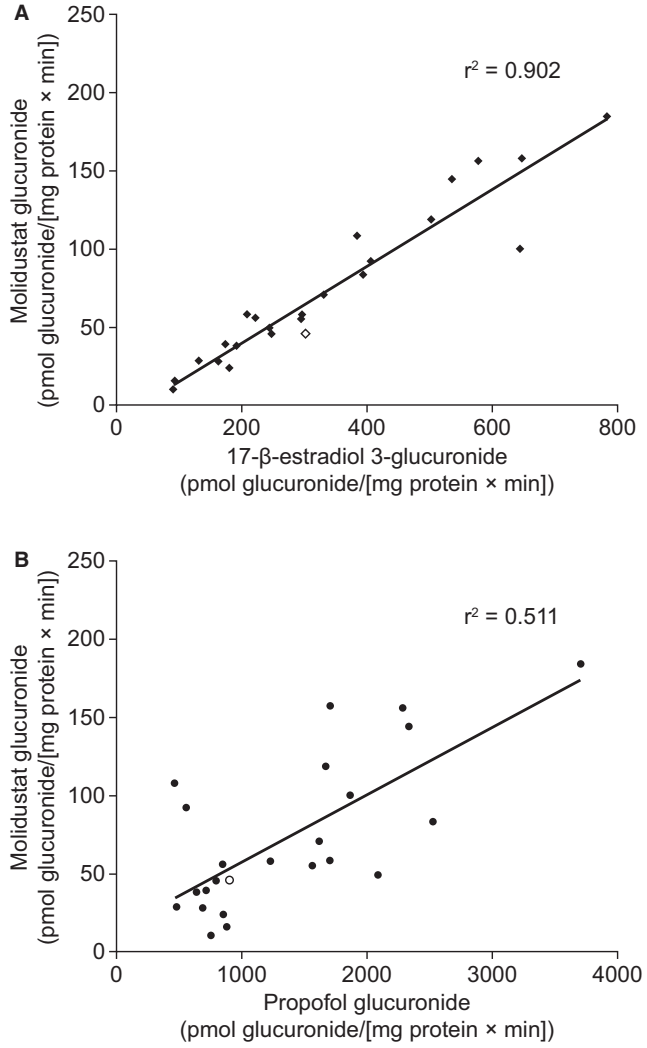

FIGURE 1 Correlation analysis (least-squares linear regression) for glucuronidation velocity of molidustat versus the isotype-specific substrates (A) 17β-estradiol for UGT1A1 and (B) propofol for UGT1A9, as observed in 23 individual (closed symbols) or one pooled human liver microsomes (open symbols). Note. UGT, 5'-diphospho-glucuronosyltransferase

with high concentrations of atazanavir (~70% inhibition). Furthermore, using reported k_a values of 0.024 min^{-1} for slow absorbers and 0.108 min^{-1} for fast absorbers [29] resulted in a predicted increase in molidustat AUC of 2.4- and 2.9-fold, respectively. Based on these findings, the in vivo DDI study was planned to verify the in vitro predictions for molidustat with concomitant atazanavir dosing.

3.2 | Clinical DDI study

3.2.1 | Participants

In total, 29 participants were screened, of which 14 passed screening and were treated according to protocol and completed the study; however, after finishing both treatments, one participant was found to be participating in a second clinical trial in parallel and was, therefore, excluded from PK, PD and per-protocol (PP) study populations because effects of other study medication could not be ruled out. All 13 participants in the PK, PD and PP analysis set were white men with a mean age of 33.1 years (range: 20-45 years), BMI of 24.9 kg m^{-2} (19.8-29.3 kg m^{-2}), height of 182 cm (168-200 cm) and weight of 82.5 kg (63.5-101 kg).

3.2.2 | Pharmacokinetic results

Plasma concentration-time profiles for molidustat and M1 (geometric means and geometric standard deviation [SD]) are given in Figure 2. For the parent compound, mean concentrations were higher with concomitant atazanavir than with molidustat alone, but the overall shape of the concentration-time profile was similar; this indicates lack of relevant effect of atazanavir on the terminal elimination characteristics. The stick plot for AUC of molidustat alone or with concomitant atazanavir (Figure 3) illustrates the general trend for a substantial increase in exposure in all participants with concomitant atazanavir. Descriptive statistical summaries of PK parameters obtained for molidustat and M1 are given in Table 3, including the results from exploratory ANOVA for AUC, AUC(0-t_{last}) and C_{max} of molidustat. Results confirmed a significant increase of approximately 100% in exposure for molidustat, as point estimates for treatment ratios were 2.07 (90% confidence interval [CI]: 1.87-2.29), 2.08 (1.88-2.29) and 2.07 (1.53-2.79) for AUC, AUC(0-t_{last}) and C_{max}, respectively. At the same time, AUC and C_{max} for M1 were slightly reduced (AUCR: 0.85 and 0.80, respectively). No effect of atazanavir on t_{max} or terminal half-life was observed for both analytes (Figure 2).

PK parameters obtained for atazanavir following the 400 mg once daily (qd) dose received 30 minutes after a light breakfast on day 5 are given in Table S7. Trough concentrations (24 hours after administration) obtained on days 2 and 3 before molidustat administration indicated an increase but, from day 4 onwards, concentrations were comparable, indicating that steady state was reached. Moreover, plasma concentrations observed in the present study were similar to the exposure reported previously.[30,31]

3.2.3 | Pharmacodynamic results

Baseline values of EPO concentration were similar for both treatments at 8.0 IU L^{-1} and 8.2 IU L^{-1} (geometric mean), respectively, and corresponding CVs were 44.6% and 43.7%, respectively. Although the overall shape of the concentration-time profiles (geometric mean and geometric SD) for EPO was similar for both treatments, the mean EPO concentrations

after dosing were slightly higher in the concomitant treatment with atazanavir compared with molidustat alone (Figure 2C). Geometric mean EPO concentrations increased by 6 hours after administration in both treatments and reached mean peak concentrations at 10 hours after dosing for the treatment molidustat alone (18.9 IU L^{-1}) and 6 hours after dosing for the treatment molidustat + atazanavir (22.6 IU L^{-1}). For both treatments, mean EPO concentrations returned close to baseline values at 24 hours after dosing.

A slightly higher EPO C_{max} was observed in concomitant treatment with atazanavir (23.9 IU L^{-1}) compared with molidustat alone (20.5 IU L^{-1}) and for the ratio to baseline-corrected factors were 2.91 (CV: 22.6%) compared to 2.56 (CV: 23.8%), respectively (Table 4). The ANOVA resulted in treatment ratios for absolute concentrations and ratio to baseline-corrected values of 1.17 (90% CI: 1.04-1.31) and 1.14 (90% CI: 1.00-1.30), respectively, indicating a minor increase of EPO response after treatment with atazanavir. Regarding EPO AUC(0-24), also a slightly higher mean value was observed, 423 IU L^{-1}*h compared to 365 IU L^{-1}*h (Table 4), and ANOVA resulted in point estimates for treatment ratios of 1.16 (90% CI: 1.06-1.27) for absolute concentration data and 1.34 (90% CI: 1.12-1.61) for baseline-corrected data.

3.2.4 | Safety results

Safety evaluation was performed on the safety analysis set that included all 14 participants treated with molidustat. The study drugs were well tolerated; all treatment-emergent AEs observed are summarized in Table 5. No severe or serious AEs related to molidustat or the combination with atazanavir occurred. Treatment-emergent AEs were only observed for the combination of molidustat and atazanavir, for example, the well-known effect of atazanavir on hepatic conjugation of bile acids (hyperbilirubinemia), which was observed in three participants. All AEs resolved by the end of the observation period without therapy being necessary.

4 | DISCUSSION

The mass balance study for molidustat confirmed that about 85% of an oral dose is cleared as N-glucuronide M1 in urine, with minor excretion of unchanged molidustat (~4% via urine; ~6% via faeces).[12] Based on the current in vitro data, including the correlation analysis, UGT1A1 is considered to be the major metabolizing enzyme of molidustat to yield M1, whereas conjugation via UGT1A9 is of minor importance. Comparable correlation analysis with isotype-specific substrates used for identification of relevant UGT isoforms has been used in the past for characterization of biotransformation of xenobiotics.[32]

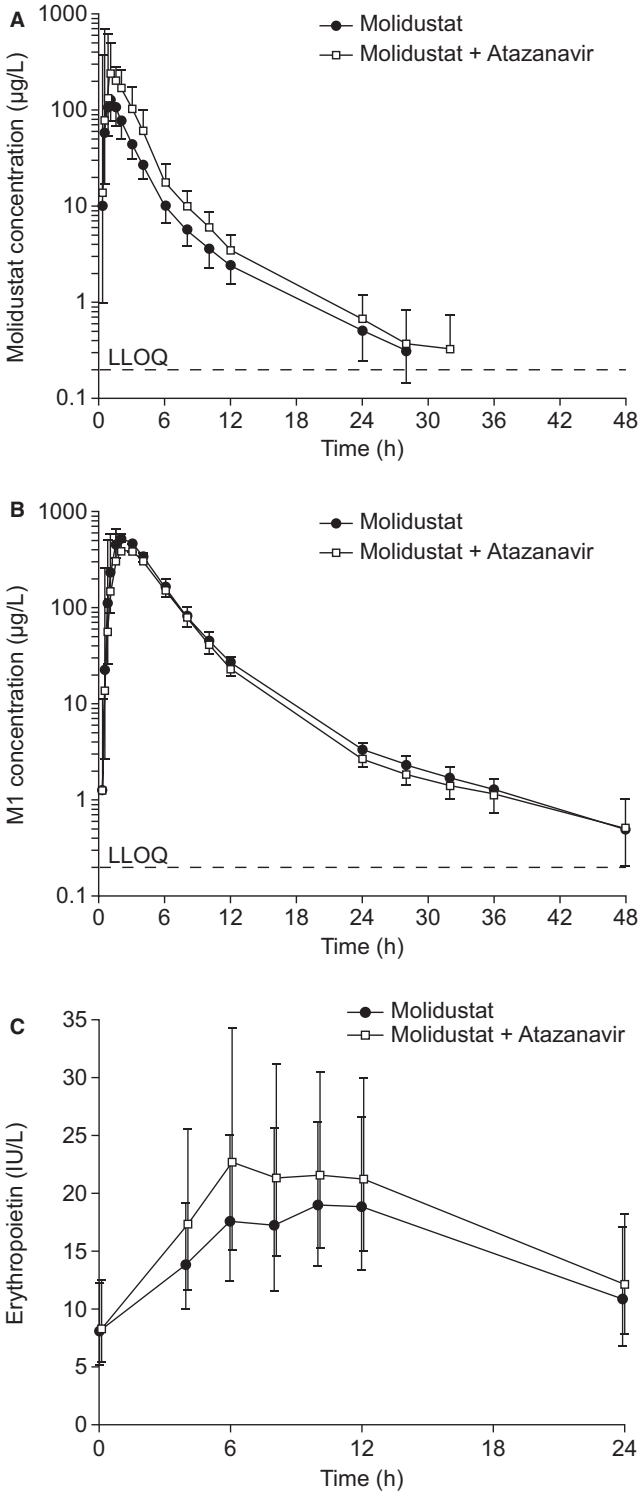

FIGURE 2 Concentration-time profile for (A) molidustat in plasma, (B) primary glucuronide metabolite M1 in plasma and (C) endogenous erythropoietin in serum, following a single, oral, immediate-release dose of 25 mg molidustat alone (part 1, filled symbols) or after 4-day pre-treatment and concomitant intake of 400 mg atazanavir qd (part 2, open symbols) to healthy males (geometric mean and SD, n = 13). Note. SD, standard deviation; qd, once daily

An extensive in vitro DDI screening using HLMs revealed several potential inhibitors of the N-glucuronidation of molidustat via UGT1A1. Like our results, the high inhibitory potency of tyrosine kinase inhibitors, including erlotinib, sorafenib, lapatinib, axitinib and imatinib, has been reported for UGT1A1.[33-36] Furthermore, clinically relevant DDIs with drugs predominantly cleared via UGT1A1 were predicted previously for erlotinib based on AUC ratios.[37]

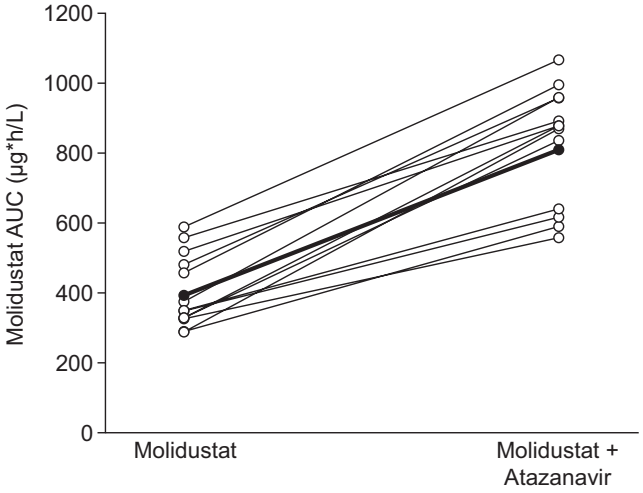

FIGURE 3 Stick plot for AUC of molidustat following a single, oral, immediate-release dose of molidustat 25 mg alone (part 1) or after 4-day pre-treatment and concomitant intake of 400 mg atazanavir qd (part 2) to healthy males (individual data and geometric mean [filled circles/bold], n = 13). Note. AUC, area under plasma concentration-time curve from zero to infinity; qd, once daily

Owing to the in vitro results indicating potential DDIs mediated by UGT1A1, the effects of inhibitory co-medication on the PK and PD of molidustat were evaluated. The predominant role of hepatic UGT1A1 found for molidustat is in line with the established characteristics of glucuronidation of xenobiotics, although intestinal and renal involvement appears to be limited.[38] Atazanavir was chosen as a relevant UGT1A1 inhibitor for the clinical DDI study based on its established use for UGT1A1 DDI studies and the prediction from in vitro data that AUC for molidustat could increase approximately by a factor of 2- to 3-fold.

In the clinical DDI study, pre- and co-treatment with atazanavir resulted in a twofold increase of AUC for molidustat, supporting the assumptions made from the in vitro-in vivo correlation regarding predominant clearance of molidustat via UGT1A1-mediated conjugation. However, the exposure to the major metabolite M1 was still approximately 85% in the presence of atazanavir, indicating that UGT1A1 activity might be reduced in the presence of atazanavir, but not completely inhibited.

TABLE 3 Pharmacokinetic parameters of molidustat (single dose, 25 mg IR tablet) and its glucuronide (M1) in healthy males after administration alone and after pre-/co-treatment with atazanavir 400 mg qd for 5 days (geometric mean/CV%), including point estimates and 90% CIs for ratios between treatments (selected parameters)

					90% CI	
Parameter	**Unit**	**Molidustat (n = 13)**	**Molidustat + atazanavir (n = 13)**	**Point estimate parameter ratio[a]**	**Lower limit**	**Upper limit**
Molidustat						
AUC	µg*h L^{-1}	393/25.3	813/22.1	2.0665	1.8674	2.2869
AUC(0-t_{last})	µg*h/L	390/25.2	810/22.1	2.0766	1.8792	2.2947
CL/F	L h^{-1}	63.6/25.3	30.8/22.1			
C_{max}	µg L^{-1}	215/38.2	444/38.1	2.0689	1.5343	2.7898
$t_{1/2}$	H	6.26/46.1	6.89/54.7			
t_{max}[b]	H	0.75 (0.25-2.0)	0.75 (0.25-3.0)			
Molidustat glucuronide (M1)						
AUC	µg*h L^{-1}	2650/13.1	2240/12.3	0.8472	0.8173	0.8781
AUC(0-t_{last})	µg*h L^{-1}	2630/13.3	2230/12.3	0.8470	0.8168	0.8783
C_{max}	µg L^{-1}	576/21.4	461/12.1	0.8002	0.7426	0.8623
$t_{1/2}$	H	9.86/53.9	11.1/37.2			
t_{max}[b]	H	2.0 (1.0-3.0)	2.0 (1.5-4.0)			

Note.: AUC, area under plasma concentration-time curve from zero to infinity; AUC(0-t_{last}), area under the plasma concentration-time curve from zero to the time of the last quantifiable concentration; CI, confidence interval; CL/F, total body clearance of drug calculated after extravascular administration (eg apparent oral clearance); C_{max}, maximum plasma concentration; CV%, coefficient of variation; qd, once daily; $t_{1/2}$, apparent terminal half-life; t_{max}, time to maximum plasma concentration.

[a](Molidustat + atazanavir)/molidustat.

[b]Median and range.

TABLE 4 Erythropoietin absolute concentrations, as well as baseline-corrected concentrations, after intake of a single oral immediate-release tablet dose of 25 mg molidustat in healthy males alone and after pre- and co-treatment with 400 mg atazanavir qd

Parameter	N	Geometric mean/CV%	Arithmetic mean ± SD	Range
C_{max}				
Absolute EPO concentration, IU L^{-1}				
Molidustat	13	20.5/33.5	21.5 ± 6.23	11.5-31.1
Molidustat + atazanavir	13	23.9/41.8	25.8 ± 11.3	13.2-55.8
Difference to baseline, IU L^{-1}				
Molidustat	13	-	12.8 ± 4.02	5.60-18.6
Molidustat + atazanavir	13	-	16.9 ± 8.28	8.25-37.9
Ratio to baseline				
Molidustat	13	2.56/23.8	2.62 ± 0.578	1.59-3.34
Molidustat + atazanavir	13	2.91/22.6	2.98 ± 0.715	2.08-4.80
AUC(0-24)				
Absolute EPO concentration, IU L^{-1}*h				
Molidustat	13	365/35.8	385 ± 121	197-578
Molidustat + atazanavir	13	423/37.0	448 ± 161	223-827
Difference to baseline, IU L^{-1}				
Molidustat	13	164/45.7	177 ± 67.1	61.6-293
Molidustat + atazanavir	13	220/38.2	234 ± 88.3	124-396
t_{max}				
Time, h				
Molidustat	13	10.0[a]	-	6.00-12.0
Molidustat + atazanavir	13	8.00[a]	-	4.0-12.0

Note.: -, not determined; $AUC_{0\text{-}24}$, area under the plasma concentration-time curve from zero to 24 hours; C_{max}, maximum plasma concentration; %CV, coefficient of variation; EPO, erythropoietin; qd, once daily; SD, standard deviation; t_{max}, time to maximum plasma concentration.

[a]Median.

TABLE 5 Number of participants experiencing treatment-emergent adverse events after intake of a single oral dose of 25 mg molidustat with or without pre- and co-treatment with atazanavir (400 mg qd for 5 days, n = 14)

MedDRA primary system organ class preferred term	Molidustat (n = 14)	Molidustat + Atazanavir (n = 14)
Participants with ≥ 1 TEAE, n (%)	0	4 (28.6)
Gastrointestinal disorders		
Abdominal pain	0	1 (7.1)
Hepatobiliary disorders		
Jaundice	0	3 (21.4)[a]
Nervous system disorders		
Headache	0	1 (7.1)

Note.: MedDRA, Medical Dictionary for Regulatory Activities; qd, once daily; TEAE, treatment-emergent adverse event.

[a]Considered by investigator to be related to atazanavir.

Given that the concentration-time profile of molidustat was shifted upwards in a parallel fashion and terminal half-life of molidustat was only marginally increased in the presence of the UGT1A1 inhibitor atazanavir (6.9 hours vs 6.3 hours), a relevant change in systemic clearance is unlikely. The absolute bioavailability of molidustat following IR tablet administration has been reported to be 59%.[12] Therefore, the increase in exposure observed with atazanavir is likely due to increased bioavailability rather than to a decrease in systemic clearance. Several publications have indicated that glucuronidation in the liver occurs mainly in the perivenous hepatocytes and less frequently in the periportal hepatocytes.[39-41] Considering the low UGT activity in the periportal zone and the high atazanavir and molidustat concentrations coming from the portal vein, it can be assumed that only the UGTs in the periportal zone can be relevantly inhibited by atazanavir. However, the activity of the

UGTs in the perivenous hepatocytes is less affected. This might explain the influence of atazanavir on pre-systemic clearance and the lack of any effect on systemic clearance.

Historically, there has been only a minor fraction of marketed drugs relying on UGTs as the predominant/exclusive clearance pathway; therefore, DDIs via UGT have been of limited clinical relevance.[38] However, recent data indicate that some new drugs are significantly cleared via UGTs. For danirixin, it has been found that approximately 90% of the drug is excreted as glucuronides, with 80% being recovered as directly conjugated parent compound without having undergone oxidative metabolism.[42] Likewise, dolutegravir is mainly cleared via UGT1A1-mediated glucuronidation, which was sensitive to atazanavir co-medication with an effect comparable to that described here on molidustat PK at a dose of 400 mg qd.[43]

Recently, it could be shown for atazanavir and raltegravir that, in healthy participants and patients, this combination at therapeutic doses resulted in increased exposure to raltegravir (eg ~70% in mean AUC for single-dose raltegravir 100 mg when given with multiple doses of atazanavir 400 mg), with a clear correlation of exposure for both drugs (ie high AUC for atazanavir resulted in about twofold higher exposure of raltegravir).[44-47] For the DDI study reported here, no correlation of atazanavir AUC with exposure of molidustat could be found, which might indicate sufficient exposure to atazanavir to achieve maximum inhibitory effect on molidustat glucuronidation over the range of variability observed in the population of healthy, male participants included.

In addition, in this study, the consequence of increases in molidustat plasma concentrations on the PD effect of EPO increase was investigated. Notably, after a single oral dose of 25 mg molidustat the increase of molidustat C_{max} and AUC by about a factor of 2 due to atazanavir co-treatment had only minor influence on the EPO response. The concomitant intake of atazanavir increased EPO C_{max} by 17% and AUC(0-24) by 16% when compared to molidustat given alone. Coadministration of molidustat and atazanavir was well tolerated.

In the clinical setting, molidustat treatment starts from low dose and is intended for individual titration based on haemoglobin response, and such minor differences in EPO response might not translate into clinically meaningful influences on haemoglobin response. Therefore, it is thought that atazanavir can be co-administered with molidustat.

5 | CONCLUSIONS

The predominant clearance pathway for molidustat in humans following an oral dosing is N-glucuronidation via UGT1A1 and, to a lesser extent, via UGT1A9. The resulting metabolite M1 subsequently undergoes renal elimination, representing the major pathway for excretion; only negligible amounts of parent compound are cleared unchanged via urine or faeces. In total, 176 possible interaction partners were screened in vitro to identify potential inhibitors of the major clearance pathway of molidustat. Many important drugs lacked significant influence on molidustat exposure based on an in vitro-in vivo scaling approach using inhibitory potency for molidustat glucuronidation. UGT-mediated molidustat glucuronidation is potently inhibited in vitro, especially by tyrosine kinase inhibitors, as well as by HIV protease inhibitors and by tranilast. Given that atazanavir, an established UGT1A1 inhibitor, was identified as a potent inhibitor in vitro, the influence of repeated atazanavir dosing on the PK and PD of molidustat was studied in healthy participants. The observed AUC ratio of 2 for molidustat with and without inhibition of UGT1A1 by atazanavir was close to the predicted 2- to 3-fold increase from in vitro-in vivo correlation, assuming a f_m value of 0.7. Comparable effects were observed for C_{max} of molidustat (twofold increase), although only a mild reduction in systemic exposure to the glucuronide M1 was found (−15%). The effects of UGT inhibition on EPO turnover were much less pronounced than on the PK of molidustat, confirming the exposure-response relationship observed in other studies.[2,48] Molidustat administered concomitantly with atazanavir was well tolerated. Given that molidustat dosing will follow a haemoglobin-guided individual dose titration, molidustat may be administered together with atazanavir.

It is considered unlikely that other UGT inhibitors will result in a more pronounced increase in molidustat exposure, since atazanavir was identified as one of the most potent ones in vitro.

ACKNOWLEDGEMENTS

The authors thank Uwe Thuss for bioanalytical analysis of molidustat and M1, and Annette Leega and Torsten Löffler for in vitro investigations. Stefanie Kapsa is kindly acknowledged for the PK evaluation, Ann-Kristin Petersen in support of statistics and Eva-Maria Krieg for medical support of study protocol preparation. The authors thank Anna Engelen for scientific input regarding liver zonation hypothesis. Medical writing support was provided by Nicolas Bertheleme of Oxford Pharma Genesis, Oxford, UK, with funding from Bayer AG.

CONFLICT OF INTEREST

DvdM, MG, NJ, AK, SS, MR and SL are employees of Bayer AG, and KY is an employee of Bayer Yakuhin. In addition, MG, DvdM, SS and SL have stock in Bayer AG, but are not paid in stock or stock options.

ORCID

Dorina van der Mey https://orcid.org/0000-0003-2779-9388
Michael Gerisch https://orcid.org/0000-0003-3807-9036
Andreas Kaiser https://orcid.org/0000-0002-7758-6500

REFERENCES

1. Macdougall IC, Akizawa T, Berns JS, Bernhardt T, Krueger T. Effects of molidustat in the treatment of anemia in CKD. *Clin J Am Soc Nephrol*. 2019;14:28-39.
2. Böettcher M, Lentini S, Arens ER, et al. First-in-man-proof of concept study with molidustat: a novel selective oral HIF-prolyl hydroxylase inhibitor for the treatment of renal anaemia. *Br J Clin Pharmacol*. 2018;84:1557-1565.
3. Locatelli F, Fishbane S, Block GA, Macdougall IC. Targeting hypoxia-inducible factors for the treatment of anemia in chronic kidney disease patients. *Am J Nephrol*. 2017;45:187-199.
4. Gupta N, Wish JB. Hypoxia-inducible factor prolyl hydroxylase inhibitors: a potential new treatment for anemia in patients with CKD. *Am J Kidney Dis*. 2017;69:815-826.
5. Beck H, Jeske M, Thede K, et al. Discovery of molidustat (BAY 85–3934): a small-molecule oral HIF-prolyl hydroxylase (HIF-PH) inhibitor for the treatment of renal anemia. *ChemMedChem*. 2018;13:988-1003.
6. Louw EH, Chothia MY. Residual renal function in chronic dialysis is not associated with reduced erythropoietin-stimulating agent dose requirements: a cross-sectional study. *BMC Nephrol*. 2017;18:336.
7. Barger TE, Wrona D, Goletz TJ, Mytych DT. A detailed examination of the antibody prevalence and characteristics of anti-ESA antibodies. *Nephrol Dial Transplant*. 2012;27:3892-3899.
8. Flamme I, Oehme F, Ellinghaus P, Jeske M, Keldenich J, Thuss U. Mimicking hypoxia to treat anemia: HIF-stabilizer BAY 85–3934 (molidustat) stimulates erythropoietin production without hypertensive effects. *PLoS One*. 2014;9:e111838.
9. Singh AK, Szczech L, Tang KL, et al. Correction of anemia with epoetin alfa in chronic kidney disease. *N Engl J Med*. 2006;355:2085-2098.
10. Bello NA, Lewis EF, Desai AS, et al. Increased risk of stroke with darbepoetin alfa in anaemic heart failure patients with diabetes and chronic kidney disease. *Eur J Heart Fail*. 2015;17:1201-1207.
11. Pfeffer MA, Burdmann EA, Chen CY, et al. A trial of darbepoetin alfa in type 2 diabetes and chronic kidney disease. *N Engl J Med*. 2009;361:2019-2032.
12. Lentini S, van der Mey D, Kern A, et al. Absorption, distribution, metabolism and excretion of molidustat in healthy participants. *Basic Clin Pharmacol Toxicol*. 2020;127:221-233.
13. Tveden-Nyborg P, Bergmann TK, Lykkesfeldt J. Basic & clinical pharmacology & toxicology policy for experimental and clinical studies. *Basic Clin Pharmacol Toxicol*. 2018;123:233-235.
14. Zhang D, Chando TJ, Everett DW, Patten CJ, Dehal SS, Humphreys WG. In vitro inhibition of UDP glucuronosyltransferases by atazanavir and other HIV protease inhibitors and the relationship of this property to in vivo bilirubin glucuronidation. *Drug Metab Dispos*. 2005;33:1729-1739.
15. Uchaipichat V, Mackenzie PI, Elliot DJ, Miners JO. Selectivity of substrate (trifluoperazine) and inhibitor (amitriptyline, androsterone, canrenoic acid, hecogenin, phenylbutazone, quinidine, quinine, and sulfinpyrazone) "probes" for human udp-glucuronosyltransferases. *Drug Metab Dispos*. 2006;34:449-456.
16. Vietri M, Pietrabissa A, Mosca F, Pacifici GM. Inhibition of mycophenolic acid glucuronidation by niflumic acid in human liver microsomes. *Eur J Clin Pharmacol*. 2002;58:93-97.
17. Miners JO, Bowalgaha K, Elliot DJ, Baranczewski P, Knights KM. Characterization of niflumic acid as a selective inhibitor of human liver microsomal UDP-glucuronosyltransferase 1A9: application to the reaction phenotyping of acetaminophen glucuronidation. *Drug Metab Dispos*. 2011;39:644-652.
18. Mano Y, Usui T, Kamimura H. Inhibitory potential of nonsteroidal anti-inflammatory drugs on UDP-glucuronosyltransferase 2B7 in human liver microsomes. *Eur J Clin Pharmacol*. 2007;63:211-216.
19. Alkharfy KM, Frye RF. Sensitive liquid chromatographic method using fluorescence detection for the determination of estradiol 3- and 17-glucuronides in rat and human liver microsomal incubations: formation kinetics. *J Chromatogr B Analyt Technol Biomed Life Sci*. 2002;774:33-38.
20. Shimizu M, Matsumoto Y, Tatsuno M, Fukuoka M. Glucuronidation of propofol and its analogs by human and rat liver microsomes. *Biol Pharm Bull*. 2003;26:216-219.
21. Soars MG, Riley RJ, Findlay KA, Coffey MJ, Burchell B. Evidence for significant differences in microsomal drug glucuronidation by canine and human liver and kidney. *Drug Metab Dispos*. 2001;29:121-126.
22. Ito K, Iwatsubo T, Kanamitsu S, Ueda K, Suzuki H, Sugiyama Y. Prediction of pharmacokinetic alterations caused by drug-drug interactions: metabolic interaction in the liver. *Pharmacol Rev*. 1998;50:387-412.
23. Rowland M, Matin SB. Kinetics of drug-drug interactions. *J Pharmacokinet Biopharm*. 1973;1:553-567.
24. European Medicines Agency. Guideline on the investigation of drug interactions 2012. https://www.ema.europa.eu/en/documents/scientific-guideline/guideline-investigation-drug-interactions_en.pdf.
25. US Food and Drug Administration. In vitro drug interaction studies — cytochrome P450 enzyme- and transporter-mediated drug interactions guidance for industry. 2017. https://www.fda.gov/downloads/Drugs/GuidanceComplianceRegulatoryInformation/Guidances/UCM581965.pdf.
26. Yang J, Jamei M, Yeo KR, Rostami-Hodjegan A, Tucker GT. Misuse of the well-stirred model of hepatic drug clearance. *Drug Metab Dispos*. 2007;35:501-502.
27. Yang J, Jamei M, Yeo KR, Tucker GT, Rostami-Hodjegan A. Prediction of intestinal first-pass drug metabolism. *Curr Drug Metab*. 2007;8:676-684.
28. Lee B, Ji HK, Lee T, Liu KH. Simultaneous screening of activities of five cytochrome P450 and four uridine 5'-diphospho-glucuronosyltransferase enzymes in human liver microsomes using cocktail incubation and liquid chromatography-tandem mass spectrometry. *Drug Metab Dispos*. 2015;43:1137-1146.
29. US Food and Drug Administration. Reyataz, clinical pharmacology biopharmaceutics review part 4. 2003. https://www.accessdata.fda.gov/drugsatfda_docs/nda/2003/21-567_Reyataz_BioPharmr_P4.pdf.
30. US Food and Drug Administration. US label REYATAZ, Bristol Myers Squibb. 2018. https://www.accessdata.fda.gov.
31. Burger DM, Agarwala S, Child M, Been-Tiktak A, Wang Y, Bertz R. Effect of rifampin on steady-state pharmacokinetics of atazanavir with ritonavir in healthy volunteers. *Antimicrob Agents Chemother*. 2006;50:3336-3342.

32. Han DE, Zheng Y, Chen X, et al. Identification and characterization of human UDP-glucuronosyltransferases responsible for the in vitro glucuronidation of salvianolic acid A. *Drug Metab Pharmacokinet*. 2012;27:579-585.
33. Miners JO, Chau N, Rowland A, et al. Inhibition of human UDP-glucuronosyltransferase enzymes by lapatinib, pazopanib, regorafenib and sorafenib: implications for hyperbilirubinemia. *Biochem Pharmacol*. 2017;129:85-95.
34. Zhang N, Liu Y, Jeong H. Drug-drug interaction potentials of tyrosine kinase inhibitors via inhibition of UDP-glucuronosyltransferases. *Sci Rep*. 2015;5:17778.
35. Cheng X, Lv X, Qu H, et al. Comparison of the inhibition potentials of icotinib and erlotinib against human UDP-glucuronosyltransferase 1A1. *Acta Pharm Sin B*. 2017;7:657-664.
36. Lv X, Xia Y, Finel M, Wu J, Ge G, Yang L. Recent progress and challenges in screening and characterization of UGT1A1 inhibitors. *Acta Pharm Sin B*. 2019;9:258-278.
37. Liu Y, Ramirez J, House L, Ratain MJ. Comparison of the drug-drug interactions potential of erlotinib and gefitinib via inhibition of UDP-glucuronosyltransferases. *Drug Metab Dispos*. 2010;38:32-39.
38. Kiang TK, Ensom MH, Chang TK. UDP-glucuronosyltransferases and clinical drug-drug interactions. *Pharmacol Ther*. 2005;106:97-132.
39. Jungermann K, Katz N. Functional specialization of different hepatocyte populations. *Physiol Rev*. 1989;69:708-764.
40. Jungermann K. Zonation of metabolism and gene expression in liver. *Histochem Cell Biol*. 1995;103:81-91.
41. Lindros KO. Zonation of cytochrome P450 expression, drug metabolism and toxicity in liver. *Gen Pharmacol*. 1997;28:191-196.
42. Bloomer JC, Nash M, Webb A, et al. Assessment of potential drug interactions by characterization of human drug metabolism pathways using non-invasive bile sampling. *Br J Clin Pharmacol*. 2013;75:488-496.
43. Song I, Borland J, Chen S, et al. Effect of atazanavir and atazanavir/ritonavir on the pharmacokinetics of the next-generation HIV integrase inhibitor, S/GSK1349572. *Br J Clin Pharmacol*. 2011;72:103-108.
44. Cattaneo D, Ripamonti D, Baldelli S, Cozzi V, Conti F, Clementi E. Exposure-related effects of atazanavir on the pharmacokinetics of raltegravir in HIV-1-infected patients. *Ther Drug Monit*. 2010;32:782-786.
45. Krishna R, East L, Larson P, et al. Efavirenz does not meaningfully affect the single dose pharmacokinetics of 1200 mg raltegravir. *Biopharm Drug Dispos*. 2016;37:542-549.
46. Iwamoto M, Wenning LA, Mistry GC, et al. Atazanavir modestly increases plasma levels of raltegravir in healthy subjects. *Clin Infect Dis*. 2008;47:137-140.
47. Neely M, Decosterd L, Fayet A, et al. Pharmacokinetics and pharmacogenomics of once-daily raltegravir and atazanavir in healthy volunteers. *Antimicrob Agents Chemother*. 2010;54:4619-4625.
48. Lentini S, Kaiser A, Kapsa S, Matsuno K, van der Mey D. Effects of oral iron and calcium supplement on the pharmacokinetics and pharmacodynamics of molidustat: an oral HIF-PH inhibitor for the treatment of renal anaemia. *Eur J Clin Pharmacol*. 2020;76:185-197.

SUPPORTING INFORMATION

Additional supporting information may be found online in the Supporting Information section.

How to cite this article: van der Mey D, Gerisch M, Jungmann NA, et al. Drug-drug interaction of atazanavir on UGT1A1-mediated glucuronidation of molidustat in human. *Basic Clin Pharmacol Toxicol*. 2021;128:511–524. https://doi.org/10.1111/bcpt.13538